ELSEVIER

Journal of Alloys and Compounds 463 (2008) 294–301

Journal of ALLOYS AND COMPOUNDS

www.elsevier.com/locate/jallcom

Thermodynamic modeling of Mg–Ca–Ce system by combining first-principles and CALPHAD method

Hui Zhang *, Yi Wang, Shunli Shang, Long-Qing Chen, Zi-Kui Liu

Department of Materials Science and Engineering, The Pennsylvania State University, 304 Steidle Building, University Park, PA 16802, USA

Received 25 January 2007; received in revised form 27 August 2007; accepted 2 September 2007
Available online 12 September 2007

Abstract

Thermodynamic assessments of the Ca–Ce and Ce–Mg binary systems were carried out by means of the CALPHAD approach complemented by first-principles calculations. The thermodynamic description for the Mg–Ca–Ce system was obtained by combining the derived databases of the Ca–Ce and Ce–Mg systems in the present work with that of the Ca–Mg system from the literature.

Keywords: Mg–Ca–Ce; Phase equilibrium; First-principles; CALPHAD

1. Introduction

Calcium and cerium are two important alloying elements used in magnesium alloys. They contribute to the performance improvement in the creep resistance and strength of Mg alloys at elevated temperatures [1]. To understand the effects of Ca and Ce on the phase stability of magnesium alloys, a complete thermodynamic description of the Mg–Ca–Ce system is desirable. Of the three constituent binary systems of the ternary system only thermodynamic modeling of Ca–Mg [2] and Ce–Mg [3] were previously carried out, but the thermodynamic description of the Ce–Mg system was not satisfactory. In particular, the predicted enthalpies of formation of Ce–Mg compounds did not agree well with the experimental data, in addition to the significant discrepancies between prediction and experiment for the solubility ranges of fcc and bcc phases. There was no existing thermodynamic description for the Ca–Ce system.

In the present work, the thermodynamic description for the Ca–Ce binary system is obtained through the CALPHAD approach, combining the available experimental data in the literature and the first-principles results calculated in this work. The thermodynamic description for the Ce–Mg binary system was updated using the CALPHAD approach by incorporating additional experimental data [4]. The resulting thermodynamic description for the Mg–Ca–Ce system was then developed by combining the derived databases of the Ca–Ce and Ce–Mg systems from the present work with that of the Ca–Mg system in the literature [2].First-principles calculations for bcc Ca–Ce solution

The isostructural enthalpies of mixing for the bcc Ca–Ce solid solutions were calculated by means of density functional theory [5]. Random solid solution phases could not be treated precisely with the implementation of the first-principles method developed for ordered structures [6–9]. In the present work, the random structure was mimicked by a so-called special quasi-random structure (SQS). The concept of SQS was first proposed by Zunger et al. [10,11] for calculating the fcc solutions. The SQS possessed, within the given interaction ranges, the local pair and multi-site correlation functions of the corresponding random alloys. Jiang et al. and Shin et al. extended this approach to the bcc [12] and hcp [13] structures, respectively. In the present work, 16 atoms SQS [12] were employed to model the bcc Ca–Ce solid solution at three compositions of 0.25 0.50 and 0.75 mole fractions of Ce, respectively.

We employed the generalized gradient approximation (GGA) together with the projector augmented-wave (PAW) pseudopotentials as implemented in the Vienna ab initio simulation package (VASP) [6–9]. For the GGA exchange-correlation

* Corresponding author. Tel.: +1 814 8639957; fax: +1 814 8652917.
E-mail address: huz106@psu.edu (H. Zhang).

0925-8388/$ – see front matter © 2007 Elsevier B.V. All rights reserved.
doi:10.1016/j.jallcom.2007.09.020

Table 1
Enthalpies of mixing of bcc solutions

Phase	eV/atom	Enthalpy of mixing (kJ/mol)	Calculated lattice parameter (Å)	Lattice parameter (Å)
Ca	−1.902		4.40	4.50 [16]
Ce	−5.732		3.756	4.11 (1041 K) [17]
Ce (with magnetic)	−5.732		3.759	4.11 (1041 K) [17]
$Ca_{0.25}Ce_{0.75}$	−4.538	22.719		
$Ca_{0.50}Ce_{0.50}$	−3.589	21.928		
$Ca_{0.75}Ce_{0.25}$	−2.688	16.488		
$Ca_{0.25}Ce_{0.75}$ (with magnetic)	−4.585	18.208		
$Ca_{0.50}Ce_{0.50}$ (with magnetic)	−3.599	20.989		
$Ca_{0.75}Ce_{0.25}$ (with magnetic)	−2.695	15.827		

energy, we used the Perdew–Wang parameterization [14] (GGA-PW91). A constant cutoff energy of 390 eV was used. Due to the structure instability of bcc solutions only the cell volume was relaxed. The Monkhorst–Pack scheme was used for the Brillouin-zone integrations [15]. $18 \times 18 \times 18$ k-point was used for pure elements Ca and Ce, $8 \times 8 \times 6$ for $Ca_{0.25}Ce_{0.75}$ and $Ca_{0.75}Ce_{0.25}$ bcc solutions and $6 \times 6 \times 10$ for $Ca_{0.50}Ce_{0.50}$. These settings of k-point roughly correspond to a 5000 k-point meshes per reciprocal atom. For Ca, only the 4s shell was treated as valence state. For Ce, the semi-core 5s 5p shells were included as valence states. On selecting the potential for Ce, an additional test was tried between the one that had one electron frozen to the 4f state and the one that did not have electrons frozen to the 4f state. It was found that using the potential that did not have one electron frozen to the 4f state was essential to yield reasonable miscibility gap by the present modeling. In addition, more tests were performed for the bcc solutions with and without considering the magnetic contribution. It was found that considering the magnetic contribution was necessary. The calculated total energies of the bcc SQS together with experimental data [16,17] are given in Table 1. The derived enthalpies of mixing with the magnetic contribution are plotted in Fig. 1.

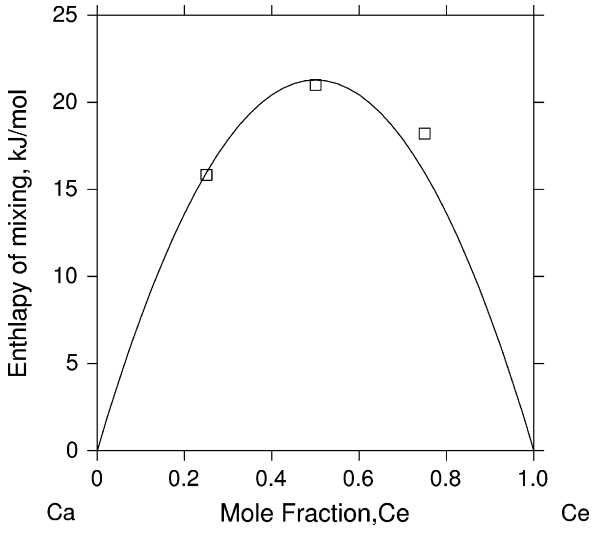

Fig. 1. Calculated enthalpy of mixing of bcc solutions at 298 K as a function of Ce concentration in the Ca–Ce system, compared with first-principles calculations (□)

3. Experimental data and previous modeling in the literature

The Ca–Mg system modeled by Zhong et al. [2] was accepted in the present work. The Ca–Ce binary system was previously studied by Zverev [18], Trombe [19] and Gschneider and Verkade [20]. Zverev [18] reported the liquidus and the mutual solubility of calcium in cerium using 99.5% Ce and 99.9% Ca. Trombe [19] observed that 1% Ca prevented Ce from forming fcc-Ce on cooling through the stabilization of bcc-Ce. The monotectic and eutectic temperatures of this system were evaluated by Gschneider and Verkade [20]. No thermochemical data of the Ca–Ce system has been reported in the literature.

Nayeb-Hashemi and Clark [21] reviewed experimental data for the Ce–Mg system. Crystal structure data for the Ce–Mg and Ca–Ce systems [22,23]are listed in Table 2. Based on the reviewed experimental data, Cacciamani et al. [3] evaluated the thermodynamic model parameters of the Ce–Mg system. However, the phase equilibria on the Ce-rich side and the liquidus of $Mg_{41}Ce_5$ were not well studied. More recently, some new experimental data on the Mg-rich and Ce-rich sides were reported in the literature [4], which could not be reproduced well by the exiting thermodynamic modeling. The Ce–Mg system thus needs to be remodeled in order to improve the agreement with experiments.

The Ce–Mg system was first studied by Vogel [24] using Ce with purity of 93.5 wt.%. Later, the phase equilibria in the composition range of 18–100 at.% Ce were re-investigated by using Ce with purity of 99.7 wt.% [25]. Liquidus curves across the phase diagram were also measured by Haughton and Schofield [26], Drits et al. [27] and Wood and Cramer [28]. The liquidus temperatures obtained by Wood and Cramer [28] is in closer agreement with those from Haughton and Schofield [26] but higher than both data from Haughton and Schofield [26] and Drits et al. [27]. In the present work, we adopted the experimental data of liquidus temperatures for alloys from 0 to 10 at.% Ce investigated by Haughton and Schofield [26] using metallography and from 0 to 15 at.% Ce obtained by Wood and Cramer [28] by differential thermal analysis, metallography and X-ray diffraction methods. The solid solubility of Ce in Mg was investigated by Haughton and Schofield [26]; by Weibke and Schmidt [29] using thermoresistometry; by

Table 2
Crystal structures of phases in the Mg–Ca–Ce system

Phase	Pearson symbol	Space groups	Strukturbericht designation	Reference
Ca	*cI*2	$Im\bar{3}m$	A2	[22]
Ce	*cI*2	$Im\bar{3}m$	A2	[22]
Mg	*hP*2	$P6_3/mmc$	A3	[22]
$Mg_{12}Ce$	*oI*338	*Im*/*mmc*	...	[23]
$Mg_{17}Ce_2$	*hP*38	$P6_3/mmc$	...	[23]
$Mg_{41}Ce_5$	*tI*92	*I*4/*m*	...	[23]
Mg_3Ce	*cF*16	$Fm\bar{3}m$	D03	[23]
Mg_2Ce	*cF*24	$Fd\bar{3}m$	C15	[23]
MgCe	*cP*2	$Pm\bar{3}m$	B2	[23]

Park and Wyman [30] using X-ray lattice parameter measurements and by Drits et al. [27], Crosby and Fowler [31] using resistivity and metallography analysis. The activity of Mg in liquid between 1083 and 1133 K was determined by Bayanov et al. [32] using vapor pressure measurements. Pahlman and Smith [33] measured the enthalpies of formation of intermetallic compounds in the system. More recently, Saccone et al. [4] prepared the Mg–94 at.% Ce alloys to determine phase equilibria between liquid and bcc, between fcc and bcc and between fcc and MgCe by Smith thermal analysis, which were not included in the previous modeling work by Cacciamani et al. [3].

4. Thermodynamic models

In this section, the thermodynamic models of two types of phases, i.e., solution phases and intermetallic compounds are presented.

4.1. Solution phases: liquid, fcc, bcc and hcp

The Gibbs energy functions of pure Ca, Ce and Mg are taken from the SGTE database [34]. The liquid, fcc, bcc and hcp solution phases are described by means of the one-sublattice model (Ca, Ce, Mg) [35]. The molar Gibbs energy can be expressed as following:

$$G_{\mathrm{m}}^{\phi} = \sum x_i^0 G_i^{\phi} + RT \sum x_i \ln x_i + {}^{xs}G_{\mathrm{m}}^{\phi} \tag{1}$$

$${}^{xs}G_{\mathrm{m}}^{\phi} = \sum_i \sum_{j>i} x_i x_j \sum_{k=0}^{n} {}^{k}L_{i,j}^{\Phi}(x_i - x_j)^k + x_{\mathrm{Ca}} x_{\mathrm{Ce}} x_{\mathrm{Mg}} I_{\mathrm{Ca,Ce,Mg}}^{\phi} \tag{2}$$

where ${}^0G_i^{\phi}$ is the molar Gibbs energy of the pure element i with the structure ϕ, ${}^{xs}G_i^{\phi}$ the excess Gibbs energy expressed in the Redlich–Kister polynomial [36] as Eq. (2) and ${}^kL_{i,j}^{\phi}$ is the kth binary interaction parameter between i and j, which may depend on temperature as $A + BT$ with A and B being the model parameters. Due to the lack of experimental data in the ternary system, the ternary interaction parameter $I_{i,j,k}^{\phi}$ is assumed to be zero.

4.2. Intermetallic phases

The compounds in the Ce–Mg system, $Mg_{12}Ce$, $Mg_{17}Ce_2$, $Mg_{41}Ce_5$, Mg_3Ce, Mg_2Ce and MgCe, are modeled as stoichiometric compounds using two-sublattice models, i.e., $(Mg)_a(Ce)_b$. Their Gibbs energy functions are described as:

$$G^{\mathrm{Mg}_a\mathrm{Ce}_b} = a^0 G_{\mathrm{Mg}}^{\mathrm{hcp}} + b^0 G_{\mathrm{Ce}}^{\mathrm{fcc}} + \Delta_{\mathrm{f}} G^{\mathrm{Mg}_a\mathrm{Ce}_b} \tag{3}$$

where ${}^0G_{\mathrm{Mg}}^{\mathrm{hcp}}$ and ${}^0G_{\mathrm{Ce}}^{\mathrm{fcc}}$ are the molar Gibbs energies of the pure element hcp Mg and fcc Ce, respectively. $\Delta_{\mathrm{f}}G^{\mathrm{Mg}_a\mathrm{Ce}_b}$ is the Gibbs energy of formation of the compound. It can be written as: $A^{\mathrm{Mg}_a\mathrm{Ce}_b} + B^{\mathrm{Mg}_a\mathrm{Ce}_b}T$, where $A^{\mathrm{Mg}_a\mathrm{Ce}_b}$ and $B^{\mathrm{Mg}_a\mathrm{Ce}_b}$ are the enthalpy and entropy of formation of the compound.

5. Evaluation of model parameters

All model parameters were evaluated using the Parrot module in Thermo-Calc software [37]. This program is able to consider all types of experimental data simultaneously. It works by minimizing the sum of errors of the collected experimental and first-principles data with given weights. The weight is chosen and adjusted based on the data uncertainties given in the original literature and the authors' judgment by analyzing the experimental procedure and considering all data at the same time. The complete thermodynamic descriptions thus obtained are shown in Tables 3 and 4 for the Ca–Ce and Ce–Mg binary systems, respectively. The reference state of the Gibbs energy of individual phase is the stable element reference (SER), i.e., the enthalpies of the pure elements in their stable states at 298.15 K and 1 bar.

In the Ca–Ce system, the evaluation of modeling parameters was started with the liquid miscibility gap and followed by the bcc phase. The thermodynamic parameter ${}^0L$ of the liquid phase requires a positive value due to the miscibility

Table 3
Thermodynamic parameters of the Ca–Ce system, in SI unit

Phase	Parameters
Liquid	${}^0L_{\mathrm{Ca,Ce}}^{\mathrm{liq}} = 44813$
bcc	${}^0L_{\mathrm{Ca,Ce}}^{\mathrm{bcc}} = 85106$
fcc	${}^0L_{\mathrm{Ca,Ce}}^{\mathrm{fcc}} = 85106$
hcp	${}^0L_{\mathrm{Ca,Ce}}^{\mathrm{hcp}} = 85106$

Table 4
Thermodynamic parameters of the Ce–Mg system in comparison with the results of Cacciamani [3], in SI unit

Phase	Cacciamani work	Present work
Liquid	${}^0L^{liq}_{Ce,Mg} = -39381.19 + 16.34052T$ ${}^1L^{liq}_{Ce,Mg} = 25338.56 - 11.86885T$ ${}^2L^{liq}_{Ce,Mg} = -15106.9$	${}^0L^{liq}_{Ce,Mg} = -36703 + 13.831T$ ${}^1L^{liq}_{Ce,Mg} = 30962 - 17.297T$ ${}^2L^{liq}_{Ce,Mg} = -15090$
bcc	${}^0L^{bcc}_{Ce,Mg} = -27000 + 3.3T$ ${}^1L^{bcc}_{Ce,Mg} = 25338.56 - 11.86885T$ ${}^2L^{bcc}_{Ce,Mg} = -15106.9$	${}^0L^{bcc}_{Ce,Mg} = -27284 + 3.641T$ ${}^1L^{bcc}_{Ce,Mg} = 25374 - 11.872T$ ${}^2L^{bcc}_{Ce,Mg} = -15094$
fcc	${}^0L^{fcc}_{Ce,Mg} = -15000 + 0.5T$ –	${}^0L^{fcc}_{Ce,Mg} = -11916 + 6.541T$ ${}^1L^{fcc}_{Ce,Mg} = -13507$
hcp	${}^0L^{hcp}_{Ce,Mg} = -94337.51 + 79.95155T$	${}^0L^{hcp}_{Ce,Mg} = -94338 + 79.952T$
$Mg_{12}Ce$	$\Delta_f G = -139880 + 84.5T$	$\Delta_f G = -182973 + 132.873T$
$Mg_{17}Ce_2$	$\Delta_f G = -217170.0 + 104.5T$	$\Delta_f G = -318800 + 215.027T$
$Mg_{41}Ce_5$	$\Delta_f G = -575000 + 299.0T$	$\Delta_f G = -832250 + 578.399T$
Mg_3Ce	$\Delta_f G = -76800 + 26.5T$	$\Delta_f G = -75046 + 25.0T$
Mg_2Ce	$\Delta_f G = -52744.6 + 15.163T$	$\Delta_f G = -44457 + 7.073T$
MgCe	$\Delta_f G = -46000.0 + 23.32T$	$\Delta_f G = -27451 + 4.401T$

Table 5
Invariant equilibria in the Ca–Ce binary system

Reaction	Experimental data		Present calculations, at.% Ce			
	T (K)	x_1 [20]	T (K)	x_1	x_2	x_3
Liquid 1 → bcc(Ce) + bcc(Ca)	1068	~99.7	1061.7	99.8	99.98	0.0015
Liquid 1 → bcc(Ca) + liquid 2	1108	~0.2	1105.8	0.27	0.023	99.97

gap, and was evaluated by using the experimental liquidus data. The thermodynamic parameters of the bcc phase were evaluated by combining the experimental data, including liquidus and monotectic and the enthalpies of mixing from first-principles calculations. The parameters of the fcc and hcp phases were set arbitrarily to be the same as in the bcc phase as it was shown that fcc, bcc and hcp have similar enthalpies of mixing [13].

The evaluation of model parameters in the Ce–Mg system began with the liquid phase followed by the bcc phase, and then the six stoichiometric compounds, fcc and hcp solution phases. Special attention was paid to liquid-bcc and bcc-fcc phase boundaries as they were not well reproduced by Cacciamani et al. [3]. The thermodynamic parameters of the stoichiometric compounds were obtained by experimental enthalpies of formation and liquidus data.

6. Results and discussions

The evaluated parameters of the Ca–Ce system in the present work are listed in Table 3. The calculated phase diagram using these parameters is shown in Fig. 2. Most of the experimental liquidus data were well reproduced. The calculated temperatures and phase compositions of the invariant reactions in the Ca–Ce system are listed in Table 5; the available experimental data are included for comparison. The degree of agreement is represented by the relative deviation formula, $\sqrt{\sum_i [(C_i - B_i)/B_i]^2/N}$, where C_i is the calculated results, B_i the experimental data and N is the amount of experimental data. The relative deviation is 30.0% between the experimental and calculated liquidus compositions for given temperatures. This large discrepancy is due to the very steep phase boundaries. The enthalpies of mixing calculated using these parameters are shown in Fig. 1 in comparison with the data from first-principles calculations. The relative deviation of enthalpy of mixing is about 6.5% between

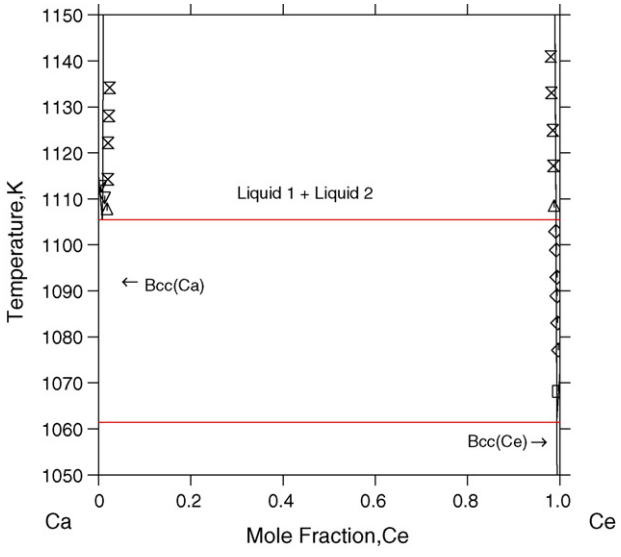

Fig. 2. Calculated Ca–Ce phase diagram compared with the experimental data (⊠) [18]; (◊) [19]; (△, □) [20].

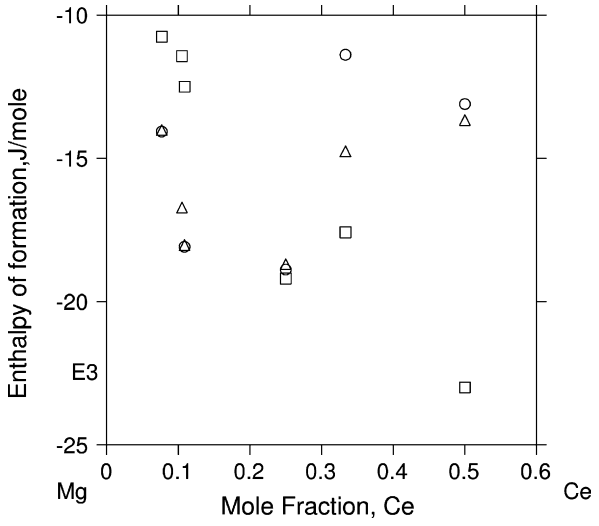

Fig. 3. Enthalpy of formation of Ce–Mg compounds (△) in comparison with the previous modeling (□) [3]and the experimental data (◯).

the first-principles results and those calculated from the present thermodynamic description.

The thermodynamic description of the Ce–Mg system obtained in the present work is listed in Table 4 in comparison with the results from Cacciamani et al. [3]. The calculated enthalpies of formation of the Ce–Mg compounds are in much better agreement with the experimental data [33] than those calculated from the previous model [3] (see Fig. 3). The relative deviation for enthalpies of formation of the Ce–Mg compounds is 12.4% in the present work and 54.1% in the previous work [3]. Fig. 4 shows the calculated vapor pressure over the Ce–Mg alloys in comparison with the experimental data [3]. The major disagreement in this figure corresponds to the measurements of alloys with 9 and 14 at.% Ce, pertaining to the $Mg_{12}Ce + Mg_{41}Ce_5$ and $Mg_{41}Ce_5 + Mg_3Ce$ phase fields identified by Pahlman and Smith [33]. In the $Mg_{12}Ce + Mg_{41}Ce_5$ phase region, it is likely that the measurements may have not reached equilibrium due to the precipitation of $Mg_{17}Ce_2$, which can be stable at high temperatures. In addition, the samples with high concentrations of Mg might be oxidized at high temperatures. For the rest of the alloys which have low concentrations of Mg, the differences between the calculations and the experiments are within the experimental uncertainties in vapor pressure measurements. As shown in Fig. 5, the calculated activities of Mg in the liquid phase agree well with experimental data [33] with the relative derivation being 5.1%, while the relative deviation is about 7.6% in the previous modeling work [3]. Fig. 6 shows the presently calculated phase diagram in comparison with that of Cacciamani et al. [3] with experimental data super-

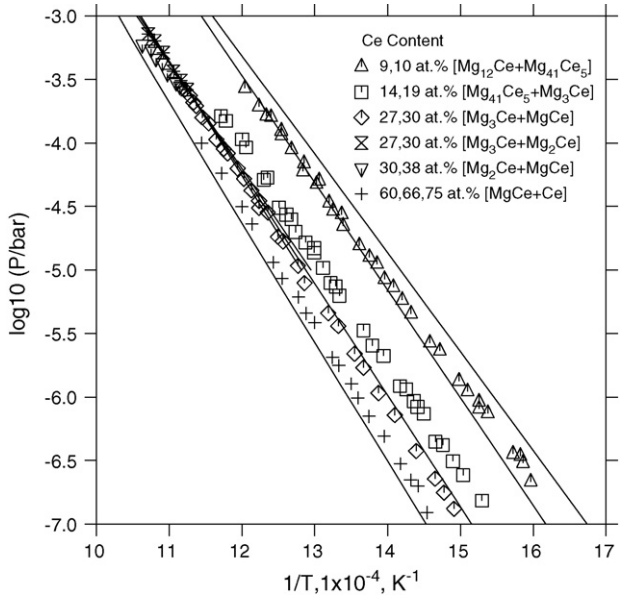

Fig. 4. Vapor pressures over Ce–Mg alloys with different Ce contents in comparison with the experimental data [33].

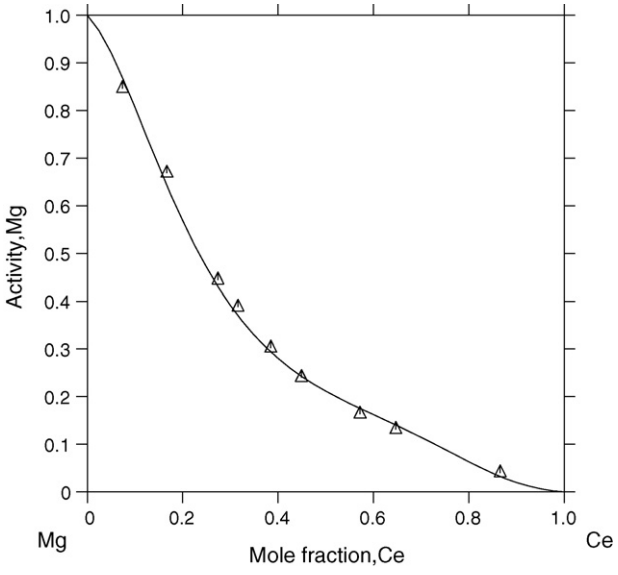

Fig. 5. Calculated activities of Mg at 1133 K in comparison with the experimental data (△) [33].

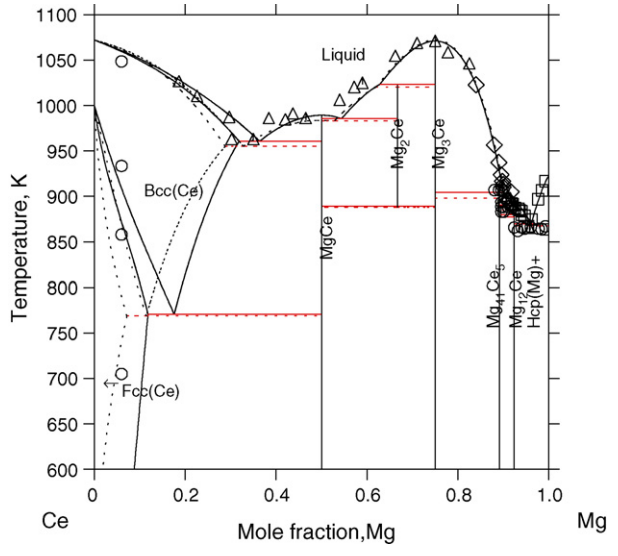

Fig. 6. Calculated Ce–Mg phase diagram in comparison with the previous modeling (dotted line) by Cacciamani et al. [3] and experimental data (□) [26]; (◊) [28]; (□) [25]; (◯) [4].

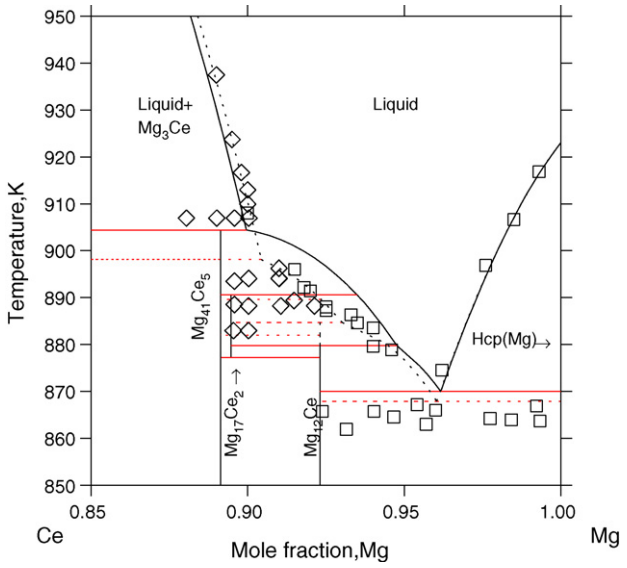

Fig. 7. Mg-rich corner of the Ce–Mg phase diagram in comparison with previous modeling (dotted line) [3] and experimental data (□) [26]; (◊) [28].

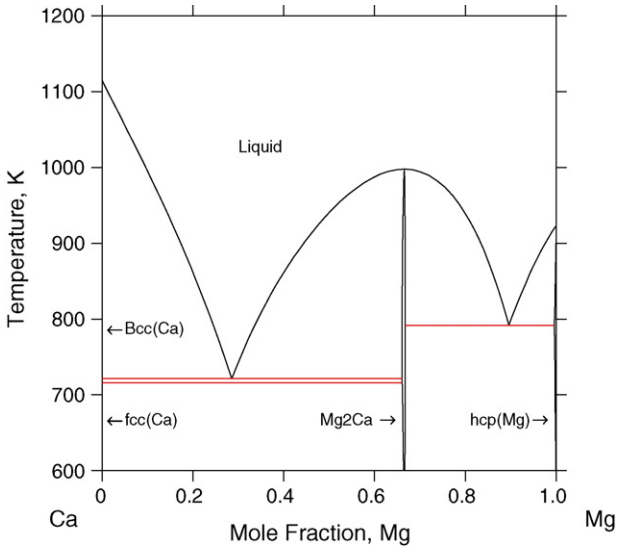

Fig. 8. Calculated Ca–Mg phase diagram using the parameters from the literature [2].

imposed. The phase diagram on the Mg-rich side is enlarged in Fig. 7. The relative deviation is 1.1% between the experimental and calculated temperatures on the phase boundaries and 10.0% between the experimental and calculated phase boundaries compositions for given temperatures. The main differences are phase equilibria at the Ce-rich side.

The present calculation reproduces the experimental data better, especially on the peritectic temperature of $Mg_{41}Ce_5$, solubility of Mg in Ce and the stability of $Mg_{17}Ce_2$ and $Mg_{41}Ce_5$. The peritectic reaction of liquid + $Mg_3Ce \rightarrow Mg_{41}Ce_5$ at about 908 K was observed by Wood and Cramer [28]. They also reported the tendency of undercooling in the temperature range from 894 to 908 K, which was illustrated by the cooling curve obtained by DTA measurements with a relatively high cooling rate of 100 °C/h [28]. Therefore, in the present work, we relied more on the experimental peritectic reaction temperature of liquid + $Mg_3Ce \rightarrow Mg_{41}Ce_5$ than those of the liquidus between liquid and $Mg_{41}Ce_5$. The calculated phase boundary has thus higher temperatures than those of experimental data in the range of 4–10 at.% of Ce. This can be further justified by considering the driving force for the formation of $Mg_{41}Ce_5$ from liquid. With the composition of $x_{Ce} = 0.09$, the calculated liquidus is at $T = 903$ K. Experimentally, the new phase was detected at $T = 896$ K [28] at which the calculated driving force is 40.77 J/mol.atom only. At a cooling rate of 100 °C/h, such a small undercooling could be expected. The invariant equilibria and congruent point in the Ce–Mg system are listed in Table 6 together with the experimental data. The relative derivation is 0.5% between the experimental invariant point temperatures and 14.7% between the experimental and calculated compositions at invariant reactions.

Fig. 8 shows the calculated Ca–Mg binary phase diagram using the parameters from the literature [38]. Fig. 9 shows the calculated liquidus projection of the Mg–Ca–Ce ternary system with the phases forming from the liquid phase during solidification. The isotherms are shown as the dotted lines with the numbers indicating the temperatures. Fig. 10 shows the liquidus projection of the Ca–Mg edge. The invariant equilibria in the liquidus projection are listed in Table 7. As an example, the calculated isothermal section of the Mg–Ca–Ce ternary system is presented in Fig. 11 at 880 K. With the thermodynamic database available, other isothermal and isopleth sections can be readily calculated.

Table 6
Invariant equilibria in the Ce–Mg binary system

Reaction	Type	Experimental data, at.% Ce				Present calculations, at.% Ce			
		T (K)	x_1	x_2	x_3	T (K)	x_1	x_2	x_3
Liquid → bcc_A2 + MgCe	Eutectic	961 [25]	65	N/A	50	960.7	63.8	6.8	50
Liquid → MgCe + Mg_2Ce	Eutectic	984 [25]	53.5	50	33.33	986.0	45.4	50	33.33
Liquid → Mg_3Ce + Mg_2Ce	Peritectic	1023 [25]	41	25	33.33	1023.3	37.2	25	33.33
Liquid + $Mg_3Ce \rightarrow Mg_{41}Ce_5$	Peritectic	908 [28]	10	25	10.87	904.4	10.0	25	10.9
Liquid + $Mg_{41}Ce_5 \rightarrow Mg_{17}Ce_2$	Peritectic	894 [28]	8.5	10.87	8.85	890.7	6.6	10.9	8.9
Liquid + $Mg_{17}Ce_2 \rightarrow Mg_{12}Ce$	Peritectic	889 [26]	7.5	8.85	7.69	880.0	6.0	8.9	7.7
Liquid → $Mg_{12}Ce$ + hcp_A3	Eutectic	865 [26]	4.3	7.69	0.09	872.0	3.8	7.7	0.03
Mg_3Ce → liquid	Congruent	1069 [25]	25			1071.0	25		

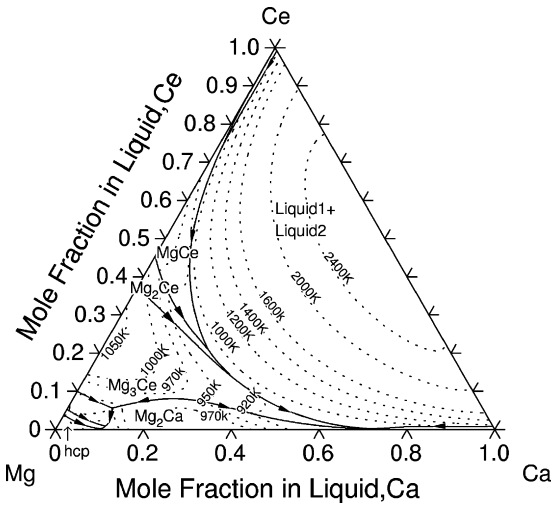

Fig. 9. Liquidus projection to the composition triangle in the Mg–Ca–Ce system.

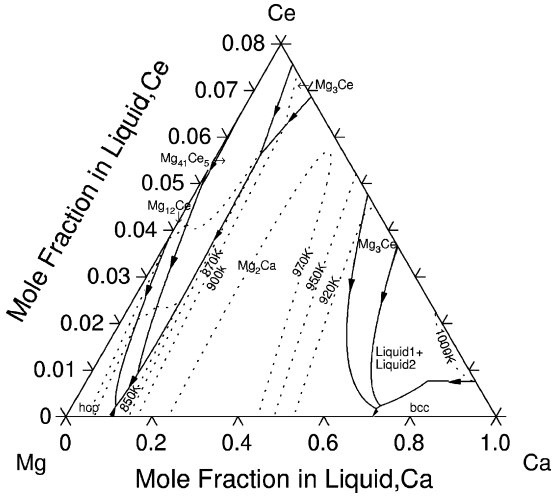

Fig. 10. Enlarged Ca–Mg edge of the liquidus projection.

7. Summary

Thermodynamic modeling of the Ce–Mg system was carried out based on the available experimental data. For the Ca–Ce system, the enthalpies of mixing from first-principles calculations were used in addition to the experimental phase equilibrium data from the literature. The thermodynamic database of the Mg–Ca–Ce ternary system was obtained by combining the thermodynamic descriptions of the presently modeled Ca–Ce and Ce–Mg systems together with the Ca–Mg system in the literature.

Table 7
Invariant reactions in the Mg–Ca–Ce liquidus projection

Reaction	Present calculations		
	T (K)	Mg (at.%)	Ce (at.%)
$MgCe + liquid\ 1 \rightarrow Mg_2Ce + liquid\ 2$	918.56	57.44	32.71
$Mg_2Ce + liquid\ 2 \rightarrow Mg_3Ce + liquid\ 1$	920.63	69.20	26.87
$Mg_3Ce + liquid\ 1 \rightarrow Mg_2Ca + Mg_{41}Ce_5$	868.81	86.75	11.22
$Mg_{41}Ce_5 + liquid\ 1 \rightarrow Mg_{12}Ce + Mg_2Ca$	820.29	88.71	9.54
$Liquid\ 1 \rightarrow Mg_2Ca + Mg_{12}Ce + hcp(Mg)$	790.30	88.30	5.57
$Mg_{17}Ce_2 + liquid\ 1 \rightarrow Mg_{41}Ce_5 + Mg_{12}Ce$	877.21	89.80	10.19
$Liquid\ 1 + liquid\ 2 + bcc(Ce) \rightarrow MgCe$	866.62	28.82	35.14
$Mg_3Ce + liquid\ 2 \rightarrow bcc(Ca) + Mg_2Ca$	720.22	58.55	11.13
$Liquid\ 1 + liquid\ 2 \rightarrow bcc(Ca) + Mg_3Ce$	766.21	51.39	23.67

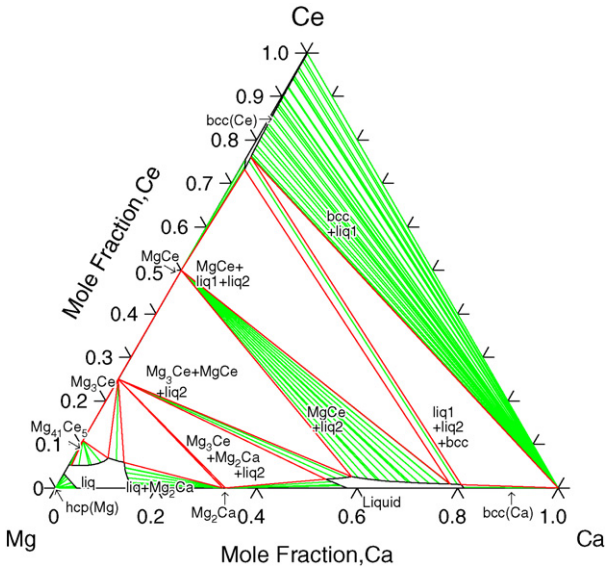

Fig. 11. Calculated isothermal section for the Mg–Ca–Ce system at 880 K.

Acknowledgements

This work is funded by the National Science Foundation (NSF) through Grant Nos. DMR-0205232 and DMR-0510180 and the United States Automotive Materials Partnership (USAMP), in whole or in part, by Department of Energy Cooperative Agreement No. DE-FC05-02OR22910. First-principles calculations were carried out on the LION clusters at the Pennsylvania State University supported in part by the NSF grants (DMR-9983532, DMR-0122638 and DMR-0205232) and in part by the Materials Simulation Center and the Graduate Education and Research Services at the Pennsylvania State University. We would also like to thank Dr. Bob R. Powell at GM for his critical reading of the manuscript and Dr. Raymundo Arroyave, Dr. Tao Wang and Dr. Dongwon Shin in our Phases Research Lab for stimulating discussions.

References

[1] G. Pettersen, H. Westengen, R. Hoier, O. Lohne, Mater. Sci. Eng. A 207 (1996) 115–120.
[2] Y. Zhong, K. Ozturk, J.O. Sofo, Z.K. Liu, J. Alloys Compd. 420 (2006) 98–106.
[3] G. Cacciamani, A. Saccone, R. Ferro, in: I. Ansara, A.T. Dinsdale, M.H. Rand (Eds.), COST 507: Thermochemical Database for Light Metal Alloys, vol. 2, European Commission, 1998, pp. 137–140.
[4] A. Saccone, D. Maccio, S. Delfino, F.H. Hayes, R. Ferro, J. Therm. Anal. Calorim. 66 (2001) 47–57.
[5] W. Kohn, L. Sham, Phys. Rev. 140 (1965) 1133–1138.
[6] G. Kresse, J. Furthmuller, Phys. Rev. B 54 (1996) 11169–11186.
[7] G. Kresse, J. Furthmuller, Comput. Mater. Sci. 6 (1996) 15–50.
[8] G. Kresse, D. Joubert, Phys. Rev. B 59 (1999) 1758.
[9] P.E. Blchl, Phys. Rev. B 50 (1994) 17953.

[10] A. Zunger, S.H. Wei, L.G. Ferreira, J.E. Bernard, Phys. Rev. Lett. (1990) 353–356.
[11] S.H. Wei, L.G. Ferreira, J.E. Bernard, A. Zunger, Phys. Rev. B 42 (1990) 9622–9649.
[12] C. Jiang, C. Wolverton, J. Sofo, L.Q. Chen, Z.K. Liu, Phys. Rev. B 69 (2004) 214202.
[13] D. Shin, R. Arroyave, Z.K. Liu, A. Van de Walle, Phys. Rev. B 74 (2006) 024204.
[14] J.P. Perdew, Y. Wang, Phys. Rev. B 45 (1992) 13244–13249.
[15] H.J. Monkhorst, J.D. Pack, Phys. Rev. B 13 (1976) 5188–5192.
[16] D.R. Lide, CRC Handbook of Chemistry and Physics, 83rd ed., CRC Press LLC, Boca Raton, FL, 2002.
[17] D.C. Koskenmaki, J.K.A. Gschneidner, in: L. Eyring (Ed.), Handbook on the Physics and Chemistry of Rare Earths: Metals, vol. 1, North-Holland Physics Publishing, Amsterdam, 1981.
[18] G.L. Zverev, Doklady Akademii Nauk SSSR 104 (1955) 242.
[19] F. Trombe, Rev. Metall. 52 (1956) 2.
[20] J.K.A. Gschneider, Rare earth alloys, D. Van Nostrand company, Inc., Princeton, NJ, 1961.
[21] A.A. Nayeb-Hashemi, J.B. Clark, Ce-Mg (Cerium-Magnesium), in: A.A. Nayeb-Hashemi, J.B. Clark (Eds.), Phase diagrams of binary magnesium alloys, ASM International, Metals Park, Ohio, 1988.
[22] J.K.A. Gschneider, F.W. Calderwood, in: L. Eyring (Ed.), Handbook on the Physics and Chemistry of Rare Earths, Intrarare Earth Binary Alloys: Phase Relationships, Lattice Parameters and Systematics, vol. 8, North-Holland Physics Publishing, Amsterdam, 1986.
[23] Q. Johnson, G.S. Smith, Acta Crystallogr. B (1970) 434–435.
[24] R. Vogel, Z. Anorg. Chem. 91 (1915) 277–298.
[25] R. Vogel, T. Heumann, Z. Metallkd. 38 (1947) 1–8.
[26] J.L. Haughton, T.H. Schofield, J. Inst. Met. 60 (1937) 339–344.
[27] M.E. Drits, Z.A. Sviderskaya, L.L. Rokhlin, Met. Metallove. 12 (1963) 143–151.
[28] D.H. Wood, E.M. Cramer, J. Less-Common Met. 9 (1965) 321–337.
[29] F. Weibke, W. Schmidt, Z. Electrochem. 46 (1940) 357–364.
[30] J.J. Park, L.L. Wyman, WACD Tech. Rep. 33 (1957) 57–504.
[31] R.L. Crosby, K.A. Fowler, United States Bureau of Mines—Reports of Investigations, 1962, p. 28.
[32] A.P. Bayanov, Yu.A. Frolov, A.Yu. Afanasev, Izv. Akad. Nauk SSSR Met. 3 (1975) 91–95.
[33] J.E. Pahlman, J.F. Smith, Metall. Trans. 3 (1972) 2423.
[34] A.T. Dinsdale, CALPHAD 15 (1991) 317–425.
[35] B. Sundman, J. Agren, J. Phys. Chem. Solids 42 (1981) 297–301.
[36] O. Redlich, A. Kister, Ind. Eng. Chem. 40 (1948) 345–350.
[37] J.O. Andersson, T. Helander, L.H. Hoglund, P.F. Shi, B. Sundman, CALPHAD 26 (2002) 273–312.
[38] Y. Zhong, A.A. Luo, J.O. Sofo, Z.K. Liu, Mater. Sci. Forum 488–489 (2005) 169–175.